Chemical Physics Letters 500 (2010) 217–222

Contents lists available at ScienceDirect

Chemical Physics Letters

journal homepage: www.elsevier.com/locate/cplett

# Zero-point energy constrained quasiclassical, classical, and exact quantum simulations of isomerizations and radial distribution functions of the water trimer using an *ab initio* potential energy surface

Gábor Czakó *, Alexey L. Kaledin, Joel M. Bowman

*Cherry L. Emerson Center for Scientific Computation and Department of Chemistry, Emory University, Atlanta, GA 30322, USA*

ARTICLE INFO

*Article history:*
Received 14 July 2010
In final form 5 October 2010

ABSTRACT

A recently suggested constrained quasiclassical trajectory (c-QCT) method for avoiding the zero-point leak in the water dimer [11] is applied to the water trimer, employing an *ab initio* full-dimensional potential energy surface. We demonstrate the failure of the standard/unconstrained QCT method for $(H_2O)_3$ and show the utility of c-QCT dynamics. In addition, standard classical molecular dynamics and c-QCT dynamics are contrasted for the time-dependence of isomerizations between the multiple global and local minima as well as radial distribution functions are obtained at low temperature and at 300 K. Results from these calculations are compared with rigorous quantum path integral Monte Carlo calculations.



## 1. Introduction

A well-known issue in classical molecular dynamics (MD) simulations is that the intramolecular vibrational zero-point energy (ZPE) is unphysically reallocated into the low-frequency intermolecular modes, which is the so-called 'zero-point leak' [1–5]. Since ZPE is not described classically this 'leak' is simply the response of system of non-linearly coupled modes to relax to the microcanonical limit. Therefore, in applications in the condensed phase ZPE is ignored and instead a purely classical phase space sampling is done. However, several applications have demonstrated the importance of ZPE in MD calculations, thus the absence of the ZPE in the standard classical MD is a significant issue [6–10]. Indeed, in gas-phase reaction dynamics calculations the quasiclassical trajectory (QCT) method is frequently used, in which the reactants have ZPE. However, the application of QCT in the condensed phase and for clusters is problematic due to the above-mentioned zero-point leak, which results in the dissociation of the cluster during the time scale of the MD simulation as we demonstrated [11] for the water dimer.

We recently proposed a practical method (see Ref. [11]) based on Refs. [1,2,12,13] for avoiding the zero-point leak in QCT calculations. The method employs 'on the fly' normal-mode analysis during the course of a trajectory and the mode energies are obtained using the normal coordinates and momenta of a minimum 'closest' to the actual structure. If the mode energy is below the corresponding ZPE (or in practice it is not in a given energy interval), the sign of the relevant normal-mode momentum is changed. After applying this constraint for each normal mode the momenta are transformed back to the Cartesian space and we continue to propagate the trajectory. In the case of the water dimer we have demonstrated that this so-called constrained QCT (c-QCT) method keeps all the mode energies close to their zero-point value for the duration of the simulation and prevents the dissociation of the dimer. We have also shown that the c-QCT gives much more realistic radial distribution functions (RDFs) for $(H_2O)_2$ than the standard classical MD when the RDFs are compared to quantum path integral [14] Monte Carlo (PIMC) results. Note that Lim and McCormack proposed another active constraint employing trajectory projection onto ZPE orbit (TRAPZ) [15]. The TRAPZ method was recently modified by Bonhommeau and Truhlar [16] applying the momentum transformation when the total instantaneous vibrational energy is below the total local ZPE.

In the present Letter, we apply the c-QCT method to the water trimer. For a detailed overview of the extensive research on the water trimer, the interested reader should consult the review written by Keutsch et al. [17]. The trimer is the smallest water cluster with a ring-like structure capturing the three-body effects, which play important role in the liquid water and ice. Furthermore, the trimer is the smallest water cluster that has multiple hydrogen bonds (H-bonds), where the H-bond rearrangement dynamics can be studied. Since the liquid water is considered as a continuously rearranging H-bonded network, the trimer ring, stabilized by three H-bonds, is an excellent model of the condensed-phase H-bonded network. Beside the c-QCT, we employ standard classical MD and quantum PIMC computations as well. In Section 2, the

* Corresponding author.
*E-mail addresses:* czako@chem.elte.hu (G. Czakó), jmbowma@emory.edu (J.M. Bowman).

0009-2614/$ - see front matter © 2010 Elsevier B.V. All rights reserved.
doi:10.1016/j.cplett.2010.10.015

computational details are given. We demonstrate the issues of the standard QCT method by monitoring the OO-distances of $(H_2O)_3$ as a function of time in Section 3, where we also discuss the isomerization and H-bond rearrangement dynamics of $(H_2O)_3$ at low temperature and 300 K. In Section 3, the RDFs obtained from different classical and quantum simulations are also presented.

## 2. Computational details

We have computed 10 constrained and 10 unconstrained QCTs for $(H_2O)_3$ using a recent *ab initio*-based full-dimensional potential energy surface (PES) denoted PES(1,2,3), which was recently developed in our group for water clusters (see Ref. [18]). All trajectories were initiated from the same global minimum. Coordinates and momenta were sampled randomly from the normal modes, in the usual way [19], with harmonic ZPE given to each normal mode for calculations at 0 K. Fixed mode energies were given by $\omega_k[1/2 + 1/(\exp(\omega_k/RT) - 1)]$ at $T = 300$ K based on the averaged energy of a harmonic quantum oscillator. Thus, these calculations are microcanonical, not canonical. We made this choice, which is commonly done, for computational convenience.

In order to apply the active constraint we need to relate each actual configuration, denoted by $\mathbf{r}_i$ ($i = 1, 2, \ldots, 9$), along the trajectory to normal mode displacements of a reference minimum geometry. In the present implementation we determine the reference geometry $[\mathbf{r}_i^{\mathrm{eq}}(i_{\min})]$ by minimizing the expression

$$\sum_{i=1}^{9} \|\mathbf{r}_i - \mathbf{C}(\theta, \phi, \psi)\mathbf{r}_i^{\mathrm{eq}}(i_{\min})\|^2 \qquad (1)$$

with respect to the three Euler angles $(\theta, \phi, \psi)$ and $i_{\min}$, where $i_{\min}$ goes through all the 96 global and 32 local minima of the trimer (see more details about the minima in Section 3). Employing the normal coordinates and momenta corresponding to the above determined reference geometry, which may vary as the system moves on the PES, the vibrational energy as well as a non-integer classical harmonic action number for each normal mode can be calculated. If an action number is not in the interval of $[-0.1, 0.1 + 1/(\exp(\omega_k/RT) - 1)]$, i.e., $[-0.1, 0.1]$ at 0 K, we apply the momentum flip for the corresponding mode. (For more details about the c-QCT method see Ref. [11].)

The total energy is about 16 000 and 17 000 $\mathrm{cm}^{-1}$ in the QCT simulations at 0 and 300 K, respectively. For both unconstrained and constrained trajectories the total integration time was roughly 17 ps. For the latter the normal-mode/energy analysis was performed at every 5th time step. A time step of 0.242 fs was used for unconstrained trajectories and a smaller time step, 0.0484 fs, was used for the constrained trajectories. (The momentum flipping is equivalent to an impulse; therefore, c-QCT requires a smaller time step to achieve good energy conservation.)

In order to demonstrate the utility of the c-QCT method and the importance of ZPE we have compared the constrained quasiclassical results to standard classical MD ones, which is commonly used for simulations in condensed phase. These standard MD trajectories were propagated for 9.2 ps after selecting 100 initial phase points $(\mathbf{p}, \mathbf{q})$ at 10 and 300 K from the normal distributions $\exp(-\mathbf{p}^2/(2mRT))$ and $\exp(-V(\mathbf{q})/RT)$ by performing a random walk at each temperature in 27 dimensions [20]. Thus the classical MD results are canonical while the c-QCT ones are microcanonical, as noted above.

The reference quantum mechanical results at 6.25 K (which provides the 0 K benchmark results, since all the modes remain in their zero-point level) and 300 K were obtained by performing PIMC simulations using the same high-quality PES as in the QCT and MD calculations. Following our previous work [11] we used $P = 2^{12}$ (6.25 K) and $P = 2^7$ (300 K) for the numerical evaluation of the density operator $\exp(-\beta\widehat{H}) = [\exp(-(\beta/P)\widehat{H})]^P$, where $\beta/P$ is the effective inverse temperature [21]. The Monte Carlo procedure was carried out using the standard Metropolis sampling methods [20] developed for PIMC simulations. In this work we utilized the staging algorithm to sample paths [22]. The number of neighboring 'beads' to be sampled simultaneously in the staging procedure was adjusted to keep the acceptance ratio around 40%; the final chosen value for the staging parameter was 12 (17) which resulted in the overall acceptance ratio of 29% (33%), at 6.25 (300) K. The RDFs (converged to within about 1% standard deviation for all atom pairs) were obtained from 12 (6.25 K) and 8 (300 K) independent PIMC calculations with each run extending to 50 000 (6.25 K) and 100 000 (300 K) imaginary time steps.

## 3. Results and discussion

As noted already, the water trimer has a ring-like structure where the monomers are connected by single H-bonds. The water dimer has only one H-bond (half H-bond/monomer), whereas in the trimer there are three H-bonds (one H-bond/monomer). Therefore, one expects that the trimer is more stable than the dimer. Indeed, the electronic dissociation energies ($D_e$) of water trimer on the PES(1,2,3) [18] (with good agreement with benchmark *ab initio* values [18]) are 10.74 and 15.72 kcal/mol for $(H_2O)_3 \rightarrow H_2O + (H_2O)_2$ and $(H_2O)_3 \rightarrow 3H_2O$, respectively, whereas the $D_e$ of $(H_2O)_2$ is 4.98 kcal/mol. However, even the 15.72 kcal/mol total dissociation energy is below the total energy in the QCT simulations (~46 kcal/mol at 0 K) and so dissociation of the trimer can certainly occur for unconstrained trajectories. Thus, we monitored the OO-distances as a function of time for constrained and unconstrained trajectories. Figure 1 shows the expectation value (averaged over 10 trajectories and the time interval $[0, t]$) of the OO-distances of $(H_2O)_3$ as a function of time. The c-QCT provides almost steady $\langle r_{ij}(\mathrm{OO})\rangle$ values, whereas the trimer begins to dissociate rapidly if no constraint is employed. Thus, Figure 1 clearly shows that standard QCT cannot be used for the water trimer and we need to apply the constrained dynamics.

There are several energetically accessible minima on the PES of the water trimer. The global minimum has three free OH in the 'down-up-up' (duu) conformation [$C_1$ symmetry and chiral], whereas the local minimum, above the global one by 0.82 kcal/

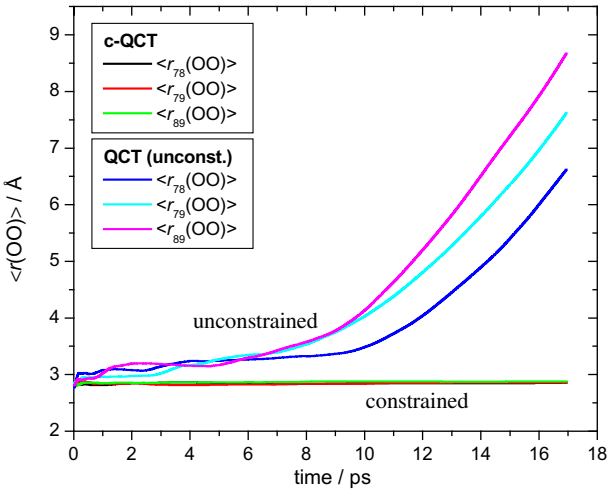


**Figure 1.** Expectation values of the OO-distances of $(H_2O)_3$ as a function of integration time obtained from constrained and unconstrained QCT (0 K) calculations initialized in the ground vibrational state of $(H_2O)_3$ using standard normal mode sampling. The $r$(OO) is averaged over 10 trajectories and the time interval $[0, t]$.

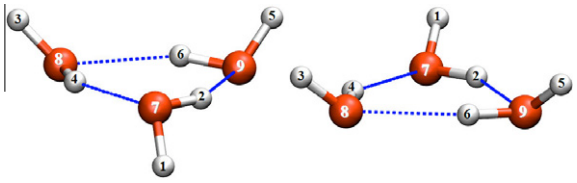

**Figure 2.** Global (left) and local (right) minima of $(H_2O)_3$.

mol [18], has (uuu) or (ddd) conformation (see Figure 2). One can obtain six equivalent global minimum configurations by the permutations of the monomers as shown in Fig. S1 of the Supplementary material. In the case of the local minimum the cyclic permutations result in the same configurations, i.e., these can be transformed to each other by overall rotation. Thus, only two distinct equivalent local minima, (ddd) and (uuu), can be obtained by monomer permutations. Furthermore, the inversion of each structure provides another set of equivalent conformations, see the structures denoted by * in Fig. S1. Finally, considering the minima shown in Fig. S1 one can get further minima by exchanging the H atoms within the monomers. Thus, $2^3 = 8$ configurations can be obtained for each structure shown in Fig. S1. Altogether there are 6 (monomer permutation) $\times$ 2 (inversion) $\times$ 8 (H atom exchange) = 96 equivalent global minima and $2 \times 2 \times 8 = 32$ equivalent local minima on the water trimer PES. (Here we do not consider the permutations of the atoms of different monomers, since the resulting configurations are separated by extremely high barrier.)

The investigation of the rearrangement dynamics between the above-described minima is an active research area [17,23,24]. One can consider three classes of motions, which connect the 96 energetically equivalent global minima of the water trimer. First, a *torsional* (*flipping motion*) connects six minima via a very low energy (0.29 kcal/mol) [18] saddle point 'up-planar-down' (upd). A single flip can be described by a cyclic monomer permutation (P) followed by an inversion (I) (through the center of mass). For example, flipping the third free OH of (duu) from up to down can be described by the following operations: $(\mathrm{duu}) \overset{\text{cyclic-P}}{\rightarrow} (\mathrm{udu}) \overset{\mathrm{I}}{\rightarrow} (\mathrm{udu})^*$, see Fig. S1. Second, the *bifurcation motion* breaks a single H-bond and a free H of the same monomer becomes H-bonded [23,24]. This is the lowest energy pathway, which connects minima by breaking H-bond through a barrier of 2.16 kcal/mol [18]. The eight minima of the trimer connected by the bifurcation motion can be obtained by exchanging H atoms within the monomers. Considering a certain minimum, three other can be accessed by single H-bond breaking, three can be obtained by double events, and one is accessed by breaking and reforming all the three H-bonds. Third, a *concerted proton transfer*, that breaks and reforms all the three H-bonds in the ring, can connect left- and right-handed trimer minima. These minima are related to each other by a non-cyclic permutation of the monomers.

In order to study the isomerization of $(H_2O)_3$ between the above-mentioned minima we consider the c-QCT and classical MD trajectories and coordinates obtained from PIMC and assign each actual configuration at time $t$ (imaginary time for PIMC) to one of the 96 global or 32 local minima, which is the 'closest' [see Eq. (1)] to the actual structure. Figure 3 shows the probability whether the assigned minimum in the time interval $[0, t]$ is the same global minimum where from the trajectory was initiated and Figure 3 also shows the time scale of the H-bond rearrangements via bifurcation motion. The distributions of the minima obtained from different simulations are presented in Figure 4. At this point a note is given regarding the PIMC distributions. Ideally, PIMC should show identical probabilities for all the equivalent minima. However, due to the fact that our path sampling does not explicitly include identical particle exchange and the number of imaginary time steps is finite, the PIMC runs can be trapped in one of the minimum wells and the PIMC distributions can depend on the starting geometry and atom labeling. On the other hand this artifact of PIMC can indicate the different pathways and barrier heights which connect a particular minimum to the others. The results presented in Figures 3 and 4 can be summarized as follows:

(i) At 10 K the classical MD shows no isomerization, the trajectory stays in the vicinity of the global minimum where from the simulation was initiated. However, the PIMC calculations show that at 6.25 K single flips do happen, which demonstrates that the classical MD does not capture the physics at very low temperatures. These flips shown by PIMC may be due to quantum mechanical tunneling, which obviously cannot be described in a classical MD simulation.

(ii) At 300 K the flips between up and down conformations are more frequent than those at very low temperatures. Classical MD and PIMC show bifurcation events at 300 K, which happen much more often in the classical simulation.

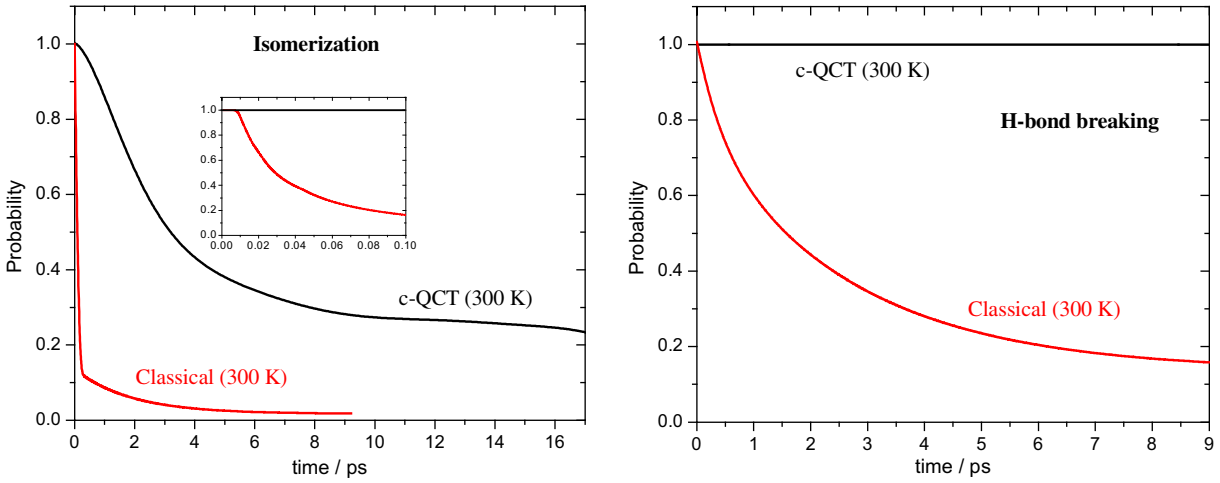


**Figure 3.** Probability of the fact that the actual configuration of $(H_2O)_3$ in the time interval $[0, t]$ is in the vicinity of the global minimum where from the trajectory was initiated (left panel) and that the H-bond structure is the same from $t = 0$ to $t$ as that was at $t = 0$ (right panel). All the trajectories were initiated from the (duu) global minimum (see Figure 2) and the left panel considers any isomerizations (flips between up and down conformations and H-bond rearrangements), whereas the right panel only shows H-bond breaking and reforming via bifurcation motion (exchange of H atoms within a monomer).

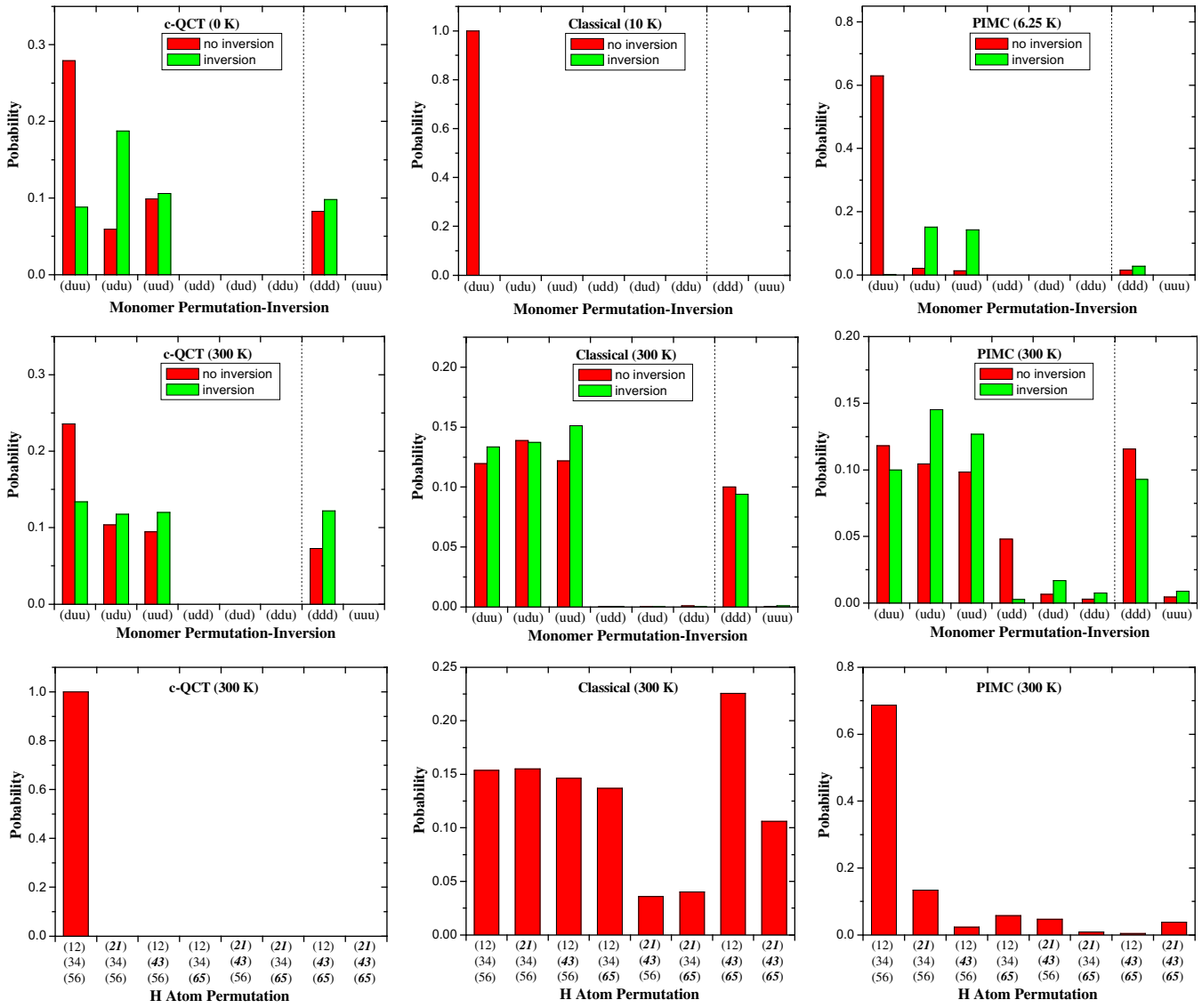


**Figure 4.** Distributions of the $(H_2O)_3$ global [(duu), . . . , (ddu)] and local [(ddd) and (uuu)] minima assigned to the actual configurations at each {imaginary} time step of the c-QCT, classical MD, and {PIMC} simulations at low temperature and at 300 K. The structures of the global and local minima (upper and middle panels) are shown in Fig. S1. The lower panels show the H atom permutations at 300 K within the monomers [(12)(34)(56) corresponds to the H atom arrangements in Figure 2]. At low temperatures we have not found exchange between free and H-bonded H atoms; therefore, the lower panels are only shown at 300 K. All the simulations were initiated from (duu) with (12)(34)(56) H atom arrangement.

(iii) At 300 K classical MD and c-QCT show that single flips occur on femtosecond and picosecond time scales, respectively. For example, considering the 0–0.1 ps time range the classical probability that $(H_2O)_3$ is in the initial configuration is less than 20%, whereas the c-QCT stays close to the initial minimum during 0.1 ps. The bifurcation motion, however, is slower by a few orders of magnitude. Classical MD at 300 K allows breaking H-bonds on a picosecond time scale, whereas it does not happen during 17 ps when the c-QCT method is employed. Averaging over 9 ps long classical (300 K) trajectories the probability of the initial H-bond arrangement (0.154) tends to its asymptotic value (1/8 = 0.125).

(iv) c-QCT and (classical MD) (almost) never sample minima which require the change of the handedness of the trimer ring via a concerted proton transfer breaking and remaking all the H-bonds. (Note that it does happen in the classical MD at 300 K, but the probability is negligible; see Figure 4.) In the case of the PIMC (300 K) we did find a small probability of minima, that have different handedness than the initial minimum. It is important to emphasize that in our study there is no H atom exchange between different monomers; thus, this concerted proton transfer shown in PIMC does not go through the pathway with barrier of 26.99 kcal/mol, which involves the breaking of covalent bonds described theoretically by Liedl and co-workers [25]. We note that the effects of this extremely high-energy motion between the left- and right-handed chiral clusters have not yet been observed in the trimer THz spectra [17].

(v) All the simulations, except classical MD at 10 K, show isomerization between local and global minima. The populations at the local minima are similar to those at the global ones. This is expected since the local minimum is only above the global one by 0.82 kcal/mol and there are low-energy saddle-points at 0.86 (upu), 0.99 (upp), and 1.47 (ppp) kcal/mol, where 'p' refers to 'planar' and the energies are relative to the global minimum [18].

Figures 5–7 show the O–O, O–H, and H–H RDFs of $(H_2O)_3$, respectively, obtained by using (a) c-QCT at 0 and (microcanonical) 300 K; (b) classical MD at 10 and 300 K; and (c) PIMC at 6.25 and 300 K. As expected, at very low temperatures (10 K in the present study) the classical MD provides RDFs with localized narrow peaks in disagreement with the quantum results even in the case of the

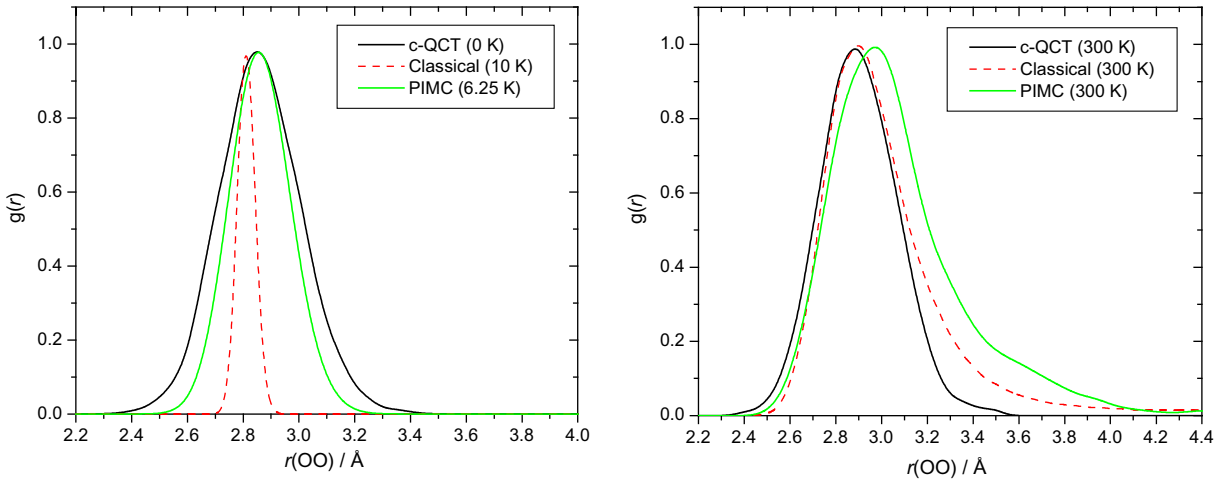


**Figure 5.** O–O RDFs of $(H_2O)_3$ obtained from c-QCT, classical MD, and quantum PIMC simulations. Each RDF is normalized having a maximum value of 1.

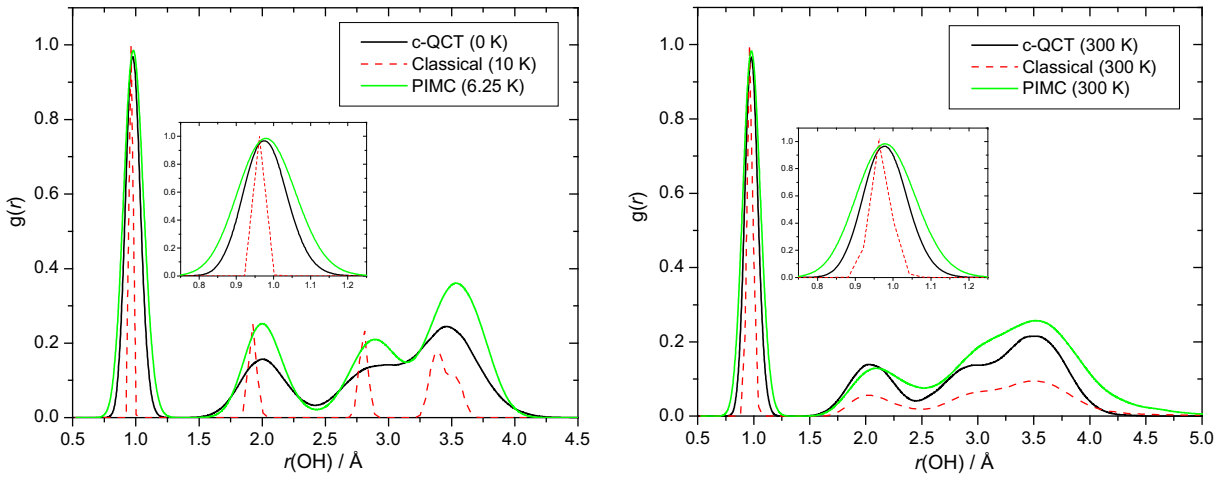


**Figure 6.** O–H RDFs of $(H_2O)_3$ obtained from c-QCT, classical MD, and quantum PIMC simulations. Each RDF is normalized having a maximum value of 1.

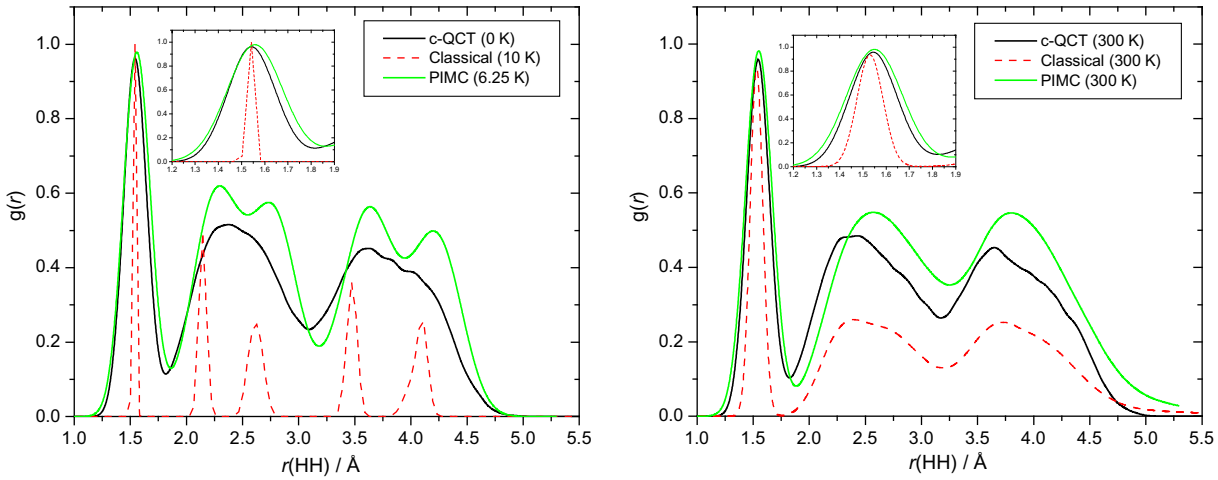


**Figure 7.** H–H RDFs of $(H_2O)_3$ obtained from c-QCT, classical MD, and quantum PIMC simulations. Each RDF is normalized having a maximum value of 1.

intermolecular distances. The positions of the peaks correspond to the different types of interatomic distances. Let us denote the trimer as $_{H1}O_7H_2\cdots{}^{H5}O_9H_6\cdots{}^{H3}O_8H_4\cdots$, where the sub- and superscript Hs correspond to the free-H atoms and the atom numbering is shown in Figure 2. In the O–H RDF plot one can identify the peaks corresponding to the (1) intramolecular OH, (2) $_{H}O\mathbf{H}_2\cdots{}^{H}\mathbf{O}_9H\cdots{}^{H}OH\cdots$, (3) $_{H}O\mathbf{H}_2\cdots{}^{H}OH\cdots{}^{H}\mathbf{O}_8H\cdots$, and (4) $_{\mathbf{H1}}OH\cdots{}^{H}OH\cdots{}^{H}\mathbf{O}_8H\cdots$ at distances of 1.0, 1.9, 2.8, and 3.4 Å, respectively. The 10 K classical H–H peaks show the (1) intramolecular HH, (2) $_{H}O\mathbf{H}_2\cdots{}^{H}O\mathbf{H}_6\cdots{}^{H}OH\cdots$, (3) $_{H}O\mathbf{H}_2\cdots{}^{\mathbf{H5}}OH\cdots{}^{H}OH\cdots$, (4) $_{H}OH\cdots{}^{\mathbf{H5}}OH\cdots{}^{H}O\mathbf{H}_4\cdots$, and (5) $_{\mathbf{H1}}OH\cdots{}^{\mathbf{H5}}OH\cdots{}^{H}OH\cdots$ distances at 1.5, 2.2, 2.6, 3.5, and 4.1 Å, respectively. The PIMC RDFs at 6.25 K display much broader distributions with slight peak features. The c-QCT (0 K) RDFs are in much better agreement with the quantum results than the classical ones demonstrating the importance of ZPE in the simulations. At 300 K the classical RDFs become significantly broader; however, they are still too narrow for the intramolecular OH and HH distances. By contrast the classical OO RDF at 300 K is in good agreement with the PIMC result, and in fact in slightly better agreement than the c-QCT RDF. Furthermore, the observed, unphysically large temperature effect in the classical MD for the intramolecular distances does not appear with c-QCT in agreement with PIMC. The c-QCT intramolecular RDFs show a negligible change between 6.25 and 300 K indicating the importance of maintaining a realistic ZPE distribution.

## 4. Summary and conclusions

The dynamics of H-bond rearrangement and radial distribution functions of the water trimer have been investigated using an accurate *ab initio*-based full-dimensional potential energy surface [18]. The dynamics studies were done using standard classical and novel constrained quasiclassical, c-QCT, approaches and radial distribution functions were obtained with these methods as well as with exact quantum path integral Monte Carlo method. We have demonstrated that the ZPE leaks into the intermolecular modes and the trimer breaks up into monomers within a few picoseconds if the standard QCT method is employed, whereas c-QCT prevents the dissociation. The time dependence of the H-bond rearrangements in the trimer using c-QCT and classical dynamics was found to be very different, with the latter being much faster than the former. The c-QCT radial distribution functions are in better agreement with the PIMC than are the standard classical ones, in agreement with previous comparisons for the water dimer [11]. The classical RDFs display narrow peak features at low temperature and too localized intramolecular OH and HH peaks even at 300 K which distributions are much broader in the c-QCT and PIMC RDFs showing the importance of the zero-point energy in the simulations.

## Acknowledgement

Financial support from the National Science Foundation (CHE-0848233) is gratefully acknowledged.

## Appendix A. Supplementary data

Supplementary data associated with this article can be found, in the online version, at doi:10.1016/j.cplett.2010.10.015.

## References

[1] J.M. Bowman, B. Gazdy, Q. Sun, J. Chem. Phys. 91 (1989) 2859.
[2] W.H. Miller, W.L. Hase, C.L. Darling, J. Chem. Phys. 91 (1989) 2863.
[3] G.H. Peslherbe, W.L. Hase, J. Chem. Phys. 100 (1994) 1179.
[4] S. Habershon, D.E. Manolopoulos, J. Chem. Phys. 131 (2009) 244518.
[5] Y. Guo, D.L. Thompson, T.D. Sewell, J. Chem. Phys. 104 (1996) 576.
[6] S. Habershon, T.E. Markland, D.E. Manolopoulos, J. Chem. Phys. 131 (2009) 024501.
[7] F. Paesani, G.A. Voth, J. Phys. Chem. B 113 (2009) 5702.
[8] J.A. Poulsen, G. Nyman, P.J. Rossky, Proc. Natl. Acad. Sci. USA 102 (2005) 6709.
[9] T.F. Miller III, D.E. Manolopoulos, J. Chem. Phys. 123 (2005) 154504.
[10] J. Liu, W.H. Miller, F. Paesani, W. Zhang, D.A. Case, J. Chem. Phys. 131 (2009) 164509.
[11] G. Czakó, A.L. Kaledin, J.M. Bowman, J. Chem. Phys. 132 (2010) 164103.
[12] G. Czakó, J.M. Bowman, J. Am. Chem. Soc. 131 (2009) 17534.
[13] G. Czakó, J.M. Bowman, J. Chem. Phys. 131 (2009) 244302.
[14] R.P. Feynman, A.R. Hibbs, Quantum Mechanics and Path Integrals, McGraw-Hill, New York, 1965.
[15] K.F. Lim, D.A. McCormack, J. Chem. Phys. 102 (1995) 1705.
[16] D. Bonhommeau, D.G. Truhlar, J. Chem. Phys. 129 (2008) 014302.
[17] F.N. Keutsch, J.D. Cruzan, R.J. Saykally, Chem. Rev. 103 (2003) 2533.
[18] Y. Wang, B.C. Shepler, B.J. Braams, J.M. Bowman, J. Chem. Phys. 131 (2009) 054511.
[19] W.L. Hase, Encyclopedia of Computational Chemistry, Wiley, New York, 1998. pp. 399–407.
[20] N. Metropolis, A.W. Rosenbluth, M.N. Rosenbluth, A.H. Teller, E. Teller, J. Chem. Phys. 21 (1953) 1087.
[21] D.M. Ceperley, Rev. Mod. Phys. 67 (1995) 279.
[22] W. Janke, T. Sauer, J. Chem. Phys. 107 (1997) 5821.
[23] F.N. Keutsch, R.S. Fellers, M.G. Brown, M.R. Viant, P.B. Petersen, R.J. Saykally, J. Am. Chem. Soc. 123 (2001) 5938.
[24] F.N. Keutsch, R.J. Saykally, D.J. Wales, J. Chem. Phys. 117 (2002) 8823.
[25] T. Loerting, K.R. Liedl, B.M. Rode, J. Chem. Phys. 109 (1998) 2672.